Palaeogeography, Palaeoclimatology, Palaeoecology
March 2024, Volume 638, Pages 112015 (10p.)
https://doi.org/10.1016/j.palaeo.2024.112015
https://archimer.ifremer.fr/doc/00869/98119/

Remote and local controls on dissolved oxygen in the Western Tropical Pacific thermocline during the last 700 kyr

Tang Zheng [1], Li Tiegang [1, 2, *], Xiong Zhifang [1, 2], Qin Bingbin [1], Li Peiying [1]

[1] Key Laboratory of Marine Geology and Metallogeny, First Institute of Oceanography, Ministry of Natural Resources, Qingdao 266061, China
[2] Laboratory for Marine Geology, Laoshan Laboratory, Qingdao 266061, China

* Corresponding author : Li Tiegang, email address : tgli@fio.org.cn

Abstract :

The dissolved oxygen level of the low-latitude Pacific thermocline is a sensitive tracer of global ocean circulation, especially at high latitudes. However, its variability covering glacial–interglacial cycles has not been well documented. Based on the thermocline-dwelling foraminiferal population extracted from Calypso Core MD06–3047, we derived a record of the Western Tropical Pacific (WTP) thermocline oxygenation over the last 700 kyr. We found that the glacial thermocline oxygenation gradually enhanced to dome-like peaks during glacial periods, with significant relative abundance of thermocline-dwelling species minimum events. We suggest that the remote physical process of lateral O2 supply (dominated by Southern Ocean (SO) ventilation and Antarctic Intermediate Water advection, with a minor contribution of North Pacific Intermediate Water (NPIW)) and the local biological process of O2 consumption (by organic biological productivity, determined by iron supply and NPIW-driven nutrient supply) may together control the WTP thermocline oxygenation on glacial–interglacial cycles. The surprisingly synchronous co-variation indicates that SO ventilation and Antarctic Intermediate Water advection have the potential to be the primary controlling factors. Furthermore, the consistent and simultaneous dramatic increments in Marine Isotope Stages 13–11 transition and each deglacial period provide robust support for a close coupling between the global (mid-Brunhes) climatic shift scenario of SO ventilation and the WTP thermocline oxygenation.

Highlights

► During glacial terminations, significant thermocline-dwelling species minimum events and dome-like enhanced oxygenation in the Western Tropical Pacific (WTP) thermocline have existed since at least ~700 ka. ► The remote physical (advection of oxygenated high latitude intermediate water) and the local biological (high productivity) processes may together control WTP thermocline oxygenation on glacial–interglacial cycles. ► Southern Ocean ventilation and the WTP thermocline oxygenation have a close coupling in global (mid-Brunhes) climatic shift scenario.

Keywords : Thermocline oxygenation, Thermocline-dwelling species minimum events, The Southern Ocean, Ventilation

Introduction

Ocean-atmosphere gas exchange plays a crucial role at glacial–interglacial (G–IG) timescales, in the global carbon cycle and variations in the partial pressure of atmospheric carbon dioxide (pCO_2^{atm}; Petit et al., 1999); this, in turn, may amplify the impact of longer-term external forcing on global climate (Sigman and Boyle, 2000). Therefore, it is proposed that changes in the Southern Ocean (SO) upwelling are crucial for regulating atmospheric CO_2 levels during glacial Terminations (Anderson et al., 2009; Menviel et al., 2018). The enhanced upwelling, perhaps associated with changes in Southern Westerlies, can stimulate the ventilation of carbon-rich deep-water masses to the surface, promoting the CO_2 outgassing and triggering global warming and glacial Termination (Skinner et al., 2010; Anderson et al., 2009).

Volumetrically, the Pacific Ocean dominates the world ocean; it is three times larger than the Atlantic Ocean; therefore, variations in its dissolved nutrient- and gas- (O_2 and CO_2) inventory represent significant changes in global ocean chemistry with potentially large impacts on climate. Simultaneously, Antarctic Intermediate Water (AAIW) mainly originates from the better-ventilated carbon-rich intermediate waters near the Sub-Antarctic Front (Bostock et al., 2013), with subsequent northward advection into the Pacific subtropical gyre through the low-latitude thermocline (Fig. 1B). Hence, AAIW can transmit the circulation and geochemical signals from deep into a tropical Pacific thermocline through the "ocean tunneling" process (Sarmiento et al., 2004; Matsumoto and Sarmiento., 2008; Bostock et al., 2010). Under current conditions, AAIW is injected into the Equatorial Pacific Intermediate Water via the South Equatorial Current and the New Guinea Coastal Undercurrent (Dugdale et al., 2002). The

dominant role of AAIW on equatorial intermediate waters was also verified by a geochemical tracer that suggests that equatorial Pacific intermediate water is primarily composed of AAIW with only a very minor contribution from the North Pacific Intermediate Water (NPIW) (Bostock et al., 2010). While the abyssal Pacific ventilation has received much attention in recent years (Jaccard et al., 2009; Bradtmiller et al., 2010) as a receiver/tracer of the SO process, the ventilation state of low-latitude Pacific thermocline remains rarely investigated and thus poorly understood.

Water oxygenation is tightly coupled with oceanic ventilation and coeval CO_2 outgassing (Nameroff et al., 2004). Similar to the reconstruction of deep carbon reservoirs based on sediment redox changes and bottom water oxygenation (Sigman and Boyle, 2000; Jaccard and Galbraith, 2012; Tang et al., 2022), the thermocline water oxygenation could provide a better understanding of the biological pump efficiency and renewal of ocean circulation in the upper water column, but its application was rare. This may be due to the lack of paleoceanographic proxies that could trace the dissolved O_2 in the thermocline of the low-latitude Pacific. The relative abundance of thermocline-dwelling *Globorotalia menardii, Pulleniatina obliquiloculata,* and *Globorotalia tumida* can reconstruct the dissolved O_2 in low-latitude thermocline (Sexton et al., 2011). All three species spend most of their life cycle within the thermocline. *G. menardii* and *P. obliquiloculata* occur in greatest abundance in the middle to upper thermocline, while *G. tumida* is found within the lower thermocline (Curry et al., 1982; Fairbanks et al., 1980; Fairbanks et al., 1982; Faul et al., 2000; Ravelo and Fairbanks, 1992; Watkins et al., 1998). The abundance patterns of these three thermocline-dwelling species

could be used to track moderately low oxygen concentrations globally in their thermocline habitat (Sexton et al., 2011). Several specific concordances between the species abundance patterns, oxygen concentrations, based on the sediment core-top database (Prell et al., 1999) and seawater oxygen concentrations (Sexton et al., 2011), support an oxygen control on these species' biogeographical distribution. The correlation between foraminifer abundance and oxygen is driven by an oxygen (or nutrient) control on the abundance of phytoplankton (e.g., diatoms, dinoflagellates), an important component of their diet (Hemleben et al., 2012). One possible link between oxygen and food supply could be that in regions with a poorly ventilated thermocline, the euphotic zone should have higher concentrations of nutrients (via entrainment and upward mixing from the underlying thermocline), fueling the production of phytoplankton (Sexton et al., 2011). Furthermore, reduced oxygen availability in a poorly ventilated thermocline (Wyrtki, 1962) should inhibit the thermocline remineralization of phytoplankton organic matter raining down from the euphotic zone, thereby encouraging the build-up of the food supply of these foraminifer species and consequent increase in relative abundance (Sexton et al., 2011).

The oxygenation of tropical Pacific thermocline remains scarcely investigated, and the physical and biological processes controlling it are still poorly understood. This pattern is controlled by gas exchange with the atmosphere at the surface and the mixing with the thermocline, transportation by the general circulation patterns in O_2-rich water, and in situ thermocline remineralization of phytoplankton organic matter raining down from the euphotic zone. On the other hand, the ventilation state of the thermocline throughout the modern low-latitude oceans

is largely dictated by the ventilation state of its higher-latitude source waters (Sarmiento et al., 2004; Toggweiler et al., 1991), a low-latitude Pacific thermocline capable of receiving SO and North Pacific signals during G–IG cycles would be expected. Furthermore, the Western Tropical Pacific (WTP) thermocline with significant carbon isotope minimum events in glacial terminations (Chen et al., 2011) has the potential to trace the advection of AAIW into low latitudes. However, whether AAIW or NPIW contributes more to the physical ventilation processes in the equatorial Pacific thermocline remains unknown.

Here, we present a proxy time-series of the WTP thermocline oxygenation variation over the last 700 kyr, using the population of thermocline dwelling *G. menardii*, *P. obliquiloculata,* and *G. tumida* extracted from the Calypso Core MD06-3047. Altogether, the combination of our faunal results with other proxy data enables the establishment of coherent paleoceanographic scenarios. Furthermore, it provides clues for the physical and biological control of low-latitude thermocline ventilation.

Material and Methods

The Calypso Core MD06-3047, 890 cm in length, was retrieved on the Benham Rise of the western Philippine Basin (17º00.44'N, 124º47.93'E) (Fig. 1A) by the Chinese-French joint cruise MARCO POLO 2/IMAGES XIV in 2006. The core was recovered from a depth of 2510 m, where it was bathed in Pacific Deep Water, a water mass whose chemical characteristics are acquired within the SO and the North Pacific (Stott et al., 2007). The bottom water is located

beneath the 27.6 kg m^{-3} isopycnal surface, which roughly divides the Upper Cell and the Lower Cell of the global meridional overturning circulation (Marshall et al., 2012). There, the subsurface thermocline waters are thought to be strongly influenced by AAIW and partially by NPIW (Tsuchiya et al., 1989). The sediment core mainly comprises yellow-brown silty clay with no evidence of turbidities or mass redeposition. A detailed description of the geological setting (e.g., topography, ocean currents, and winds) in the Philippine Sea was reported by Xu et al. (2008, 2012) and Wan et al. (2012). The Benham Rise is an oceanic plateau that formed along the Central Basin Ridge at 45–50 Ma (Hilde and Lee, 1984). The core site is located about 240 km east of Luzon. A subtropical East Asian monsoonal climate dominates the region of Luzon (Liu et al., 2009).

The core was subsampled at 2 cm intervals, and 445 samples were prepared for analysis. The dry weight of these samples was determined and divided by the wet volume of the sample to obtain the dry bulk density, which had been measured by Xu et al. (2015). After being dried at 50°C, each sample (5 g dry weight) was treated with 5% H_2O_2 and washed through a 63 μm sieve to recover the foraminiferal tests. All foraminiferal specimens were counted and identified from the dried residues. At least 300 planktonic and benthic foraminifera tests were counted in each sample.

To assess the dissolution effect, we calculated the relative abundance of the resistant species (RSP) (Cullen, 1981):*Neogloboquadrina dutertrei, G. menardii, P. obliquiloculata, Neogloboquadrina pachyderma, Globorotalia truncatulinoides, Globorotalia inflata,*

Sphaeroidinella dehiscens, *Turborotalita humilis*, *G. tumida*, *Globorotalia crassaformis* (Berger, 1975).

Results and discussion

1. Chronological framework

The chronological framework of core MD06-3047 was obtained by graphically comparing the benthic foraminifera *Cibicidoides wuellerstorfi* $\delta^{18}O$ curve from this core (Tang et al., 2013) with that of the LR04 $\delta^{18}O$ stack (Lisiecki and Raymo, 2005) and also upon consideration of the last appearance datum of *G. ruber* (pink). The last appearance datum of *G. ruber* (pink) appeared at a depth of 160 cm, with a known age of 120 ka B.P. (Thompson et al., 1979). Based on this chronology, the period of sediment accumulation spans marine isotope stages (MIS) 1–17 and thus potentially records the paleoceanographic history of the WTP over the last 700 kyr (Fig. 2).

2. Dissolved O_2 in WTP thermocline and its controlling factors

2.1 Dissolved O_2 variation in WTP thermocline during G–IG cycles

The relative abundance of specific foraminifera species is influenced by both the ecological conditions of the water above and the extent of post-depositional differential dissolution between species (Berger et al., 1976). This post-depositional dissolution process results in an enrichment of RSP and may impact the accurate assessment of the relative abundance of three thermocline species (*P. obliquiloculata, G. menardii*, *G. tumida*). In order to minimize the effects of post-depositional dissolution, we employed normative calculations to determine the relative abundance of these thermocline species in RSP (*P. obliquiloculata*/RSP, *G. menardii*/RSP, *G. tumida*/RSP and the thermocline species stack/RSP). Since these species are part of the RSP, which serves as an indicator of post-depositional dissolution (Cullen et al., 1981), our calculations assume that their relative abundance in RSP remains constant once the foraminiferal shells are deposited on the seafloor.

As a reliable tracer of moderately low oxygen concentrations in their habitat from upper to lower thermocline (Sexton et al., 2011), the relative abundances of *G. menardii*, *P. obliquiloculata*, and *G. tumida* in RSP show significant periodicity in the G–IG cycles (Fig. 3B-D). To remove interspecific differences and to obtain the entire thermocline oxygenation state, we calculated the stacked data on the relative abundance of these three thermocline species (Fig. 3E). The thermocline species stack is obtained by summing the relative abundances of three thermocline species. Leveraging the high consistency among the three relative abundances and clearer trends in the stacked data (Fig. 3B-D and E), we used the relative abundance of the three thermocline species stack/RSP as a proxy for the evolution of thermocline oxygenation (TO) conditions. Higher relative abundance values are indicative of

reduced TO, whereas lower values suggest elevated TO (Cullen et al., 1981; Sexton et al., 2011). In most glacial periods, the TO gradually enhanced; after the ice age terminations the TO developed a dome-like peak, afterwhich the oxygen levels quickly decreased during the interglacial period (Fig. 3). In each glacial Termination, the significant thermocline-dwelling species minimum events (TMEs) characterized by very low relative abundance of thermocline-dwelling species, reflect the remarkably enhanced oxygenation of the thermocline and the associated ventilation.

2.2 Controlling factors

The oxygenation of the WTP thermocline is mainly controlled by several factors related to physical and biological processes that respectively determine the supply and consumption of dissolved O_2. These factors are:

1) Physical factors

A. O_2 could be supplied by vertical mixing related to air-sea exchange and mixing in the water column. The depth of the thermocline (DOT) record could provide the vertical mixing state of the thermocline with the water column. A shallower depth of the thermocline indicates a strengthening of upper water mixing; however, thermocline deepening limits migration of O_2 from the surface to thermocline water mass, resulting in lower dissolved O_2 supplied by vertical mixing in the thermocline (Turk et al., 2001; Feely et al., 2002; Xiong et al., 2022; Guo et al., 2022).

B. O_2 could be replenished by the advection of dissolved O_2-rich AAIW and NPIW to the low-latitude thermocline. As the most important source of dissolved O_2 in global subsurface water, AAIW could propagate the O_2-rich signal to the low-latitude thermocline by SO ventilation and AAIW advection (Russell and Dickson, 2003; Spero et al., 2002; Anderson et al., 2009). In addition, the O_2-rich NPIW could also contribute to the oxygenation of the low-latitude thermocline (Bostock et al., 2010).

C. Under usual atmospheric pressure conditions, seawater dissolved O_2 saturation concentration varies with the water temperature. Therefore, the lower thermocline water temperature could contribute to increased dissolved O_2 concentration in the low-latitude thermocline.

2） Biological factors

O_2 could be consumed by the remineralization of concentrate-sinking organic matter due to the density discontinuities found across thermoclines (Karstensen et al., 2008).

To verify the contribution of these potential controlling factors to thermocline oxygenation, we compared their variation trends in G–IG cycles. In most glacial periods, the TO gradually enhanced; after the ice age terminations/TMEs with the dome-like oxygenation peaks, the TO quickly decreased during the interglacial period (Fig. 4B). During the same variation cycles, the depth of the thermocline becomes deeper and then shallower, and the thermocline water temperature rises and then falls. These conditions indicate that both vertical mixing and oxygen

solubility contribute negatively to the variation of thermocline oxygenation in factors (1A) and (1C) (Fig. 4C, D). This also implies that the other controlling factors contribute enough to the thermocline oxygenation to cover the negative contributions of the factors mentioned above.

Subsequently, we examined the control of dissolved O_2-rich AAIW and NPIW advection (in factor 1B) on thermocline oxygenation in the WTP. In G–IG cycles, the progressive enhanced TO (Fig. 5) corresponds to a gradually enhanced SO upwelling as recorded by biogenic opal and the accumulation rate in EPICA Dome C (Tang et al., 2016). However, after the optimum oxygenation during the Terminations/TMEs, the TO and SO upwelling decline rapidly and synchronously during interglacials (Fig. 5). This implies a significant positive contribution of AAIW advection to the variation of thermocline oxygenation in the WTP during glacial terminations.

However, it is important to examine whether NPIW can also significantly affect thermocline oxygenation and AAIW. Although the ventilated NPIW and AAIW are similarly enriched in oxygen, the inorganic carbon isotopes of their water masses are different. When formation and ventilation are enhanced, especially during deglaciation/TMEs, $\delta^{13}C$ becomes relatively more depleted in AAIW and more enriched in NPIW (Spero et al., 2002; Shao et al., 2020; Max et al., 2017; Zou et al., 2020). During G–IG cycles, the enhanced oxygenation and the decrease in $\delta^{13}C$ of the WTP thermocline varied roughly synchronously (Fig. 4E). During the deglacial periods/TMEs with optimum oxygenation, the $\delta^{13}C$ in the thermocline is more depleted, coinciding with the carbon isotope minimum events reflecting the enhanced ventilation in the SO (Fig. 4E; Andersen et al., 2009; Shao et al., 2020). Moreover, the low productivity during the deglacial periods/TMEs does not provide evidence to support the notion that the NPIW

(Fig. 4F), which has higher nutrient content in comparison to AAIW (Rippert et al., 2017), is the primary water-mass advection to the WTP thermocline. However, during glacial periods characterized by a weakened TO in the WTP, the AAIW experienced a decrease in strength, whereas the NPIW was enhanced (Fig. 5B,C; Andersen et al., 2009; Pichevin et al., 2009; Max et al., 2017). Althogh the AAIW and NPIW are similarly oxygen-enriched, the enhanced contribution of more nutrient-rich NPIW can provide a greater supply of nutrients to the WTP thermocline, leading to increased O_2 consumption and decreased TO in the glacial WTP (see next paragraph for detailed discussion). Therefore, the relative contribution seesaw of southern and northern intermediate waters has a notable impact on the TO in the WTP during G-IG cycles, similar to the thermocline water characteristics in the eastern equatorial Pacific (Rippert et al., 2017; Max et al., 2017).

The higher export production in the glacial WTP (as recorded by variations in the product of total organic carbon and mass accumulate rate) (Fig. 4F; Xu et al., 2015) implies that more organic matter was released from the euphotic zone, leading to an enhanced O_2 consumption in the thermocline. This is consistent with the assumptions in factor (3). The enhanced supply of nutrients caused by the increased contribution of more nutrient-rich NPIW entering the WTP thermocline, could contribute to the enhanced productivity in the glacial WTP (Fig. 4E). Furthermore, the tight correlation between variations in the dust supply and export production indicates an dust-affected O_2 consumption in the WTP thermocline (Fig. 4F, G; Xu et al., 2015). The enhanced iron-bearing dust inputs to the WTP caused by the strengthened winter monsoon

winds/Westerlies and increased aridity in Central Asia during glacial periods (Fig. 4G; Wan et al., 2012; Xu et al., 2012, 2015), might stimulate nutrient utilization and phytoplankton growth and thus enhanced O_2 consumption (Fig. 4F; Xiong et al., 2013; Xu et al., 2015). The records from the eastern and central equatorial Pacific suggest that the productivity of these areas is influenced by the upwelling of water from Equatorial Undercurrent containing dissolved iron, rather than by wind-borne dust (Winkler et al., 2016; Jacobel et al., 2019). However, in the western part of the equatorial Pacific, where the WTP is closer to the Asian continent and further away from the upwelling of the eastern equatorial Pacific, the source of dissolved iron in the upper water may vary compared to the central and eastern equatorial Pacific. Irrespective of the origin of dissolved iron in the WTP, enhanced productivity during glacial periods is frequently linked to elevated oxygen consumption and reduced dissolve O_2 in thermocline. In contrast, during deglacial and interglacial periods, the inverse pattern is observed. We suggest the remote physical process of lateral O_2 supply (dominated by SO ventilation and AAIW, with a minor contribution of NPIW) and the local biological process of O_2 consumption (by organic biological productivity, determined by iron supply and NPIW-driven nutrient supply) synergistically control the WTP thermocline oxygenation.

2.3 The deglacial dissolved O_2 peaks in the WTP thermocline

The three thermocline-dwelling species' population of core MD06-3047 is characterized by pronounced collapse during each glacial Termination (Fig. 5B), as previously mentioned TMEs,

indicating peaks in dissolved O_2 concentration. The significant deglacial dissolved O_2 peaks in the WTP thermocline resemble the carbon isotope minimum events in planktonic foraminiferas that are found in the equatorial Pacific (Spero et al., 2002; Pena et al., 2008; Chen et al., 2011) as well as in the high- and mid-latitude SO (Ninnemann et al., 2002; Ziegler et al., 2013). The consistency of TME dissolved O_2 peaks and the carbon isotope minimum events emphasizes the migration of O_2 and nutrient-laden waters to the low-latitude thermocline by intensive SO upwelling and AAIW propagation (Spero et al., 2002; Anderson et al., 2009). If the controlling factors proposed in the previous section are truly valid to explain the significant dissolved O_2 peaks in the WTP thermocline, the deglacial vigorous SO ventilation and low export productivity would be expected. The most compelling support for our hypothesis comes from the opal peaks (Fig. 5C) and low export production (Fig. 4F) during each Termination.

Conversely, O_2 solubility and vertical mixing contribute negatively to the TO peaks during deglacial TMEs (Fig. 4C, D). From the above, SO ventilation-dominated lateral O_2 advection and organic biological productivity control the supply and consumption process through a synergy of physical and biological processes, hence driving the dissolved O_2 in the WTP thermocline.

3. Role of SO ventilation in dissolved O_2 variation of the WTP thermocline

The co-variation of SO ventilation and organic biological productivity highlights our understanding of the joint control of physical and biological processes on dissolved O_2 in the

WTP thermocline. However, it remains to be shown whether the observed G–IG dissolved O_2 resulted primarily from export productivity or SO ventilation. Here, we explored the primary controlling factor in the context of the synchronization of periodic evolution. Dissolved O_2 has a cyclical variation that corresponds approximately to the G–IG cycles. After MIS 13, the start and end points of each TO decline and rise cycle (Fig. 5B) are surprisingly synchronous with the attenuation and enhancement period of the SO ventilation directly indicated by the biogenic opal (Fig. 5C; Tang et al., 2016). In the cycles before MIS 13, as the EDC accumulation rate is not a direct proxy for SO ventilation, the synchronicity was still apparent, but the correlation is weaker (Fig. 5D; WAIS, 2013). However, this remarkable synchronicity did not appear in the export productivity records (Fig. 4F; Xu et al., 2015). In addition, as the trigger of the bipolar-seesaw mechanism (Stocker et al., 2003), the synchroneity of North Atlantic freshwater injection and dissolved O_2 variation cycles provided a more robust support to the role of SO ventilation (Fig. 5E, F; Barker et al., 2015; Wright et al., 2002;).

The primary physical control on dissolved O_2 in the WTP thermocline will likely be embodied in a longer time scale. The "lukewarm" interglacials (MIS 13 to 19) and the subsequent mid-Brunhes climatic shift (MIS 12/11 transition) could provide the ideal scenario to test our hypothesis (Jansen et al., 1986). The lukewarm interglacials are characterized by a reduced amplitude of the lower atmospheric pCO_2 records and a cooler climate (Fig. 5A; Luthi et al., 2008; Jouzel et al., 2007; Lisiecki & Raymo, 2005). The muting of the pCO_2 increase during the lukewarm interglacials might have been linked to a reduced dynamic range of Antarctic overturning, thereby with a weaker SO upwelling than in more recent interglacials (Fig. 5C, D;

Russell et al., 2006; Jaccard et al., 2010, 2013). If the dissolved O_2 in the WTP thermocline is primarily controlled by SO upwelling, the deglacial maximum dissolved O_2 should be higher than the succeeding Terminations. The synchronous shift of the deglacial maximum in SO upwelling, pCO_2, and the dissolved O_2 from the lukewarm to more recent interglacials (Fig. 5), strongly suggests a robust sensitivity of dissolved O_2 in the WTP thermocline to SO physical processes.

We suggest that the physical processes (advection and lateral O_2 supply) were more vital than the biological process (export productivity), primarily controlling the dissolved O_2 in the WTP thermocline during G–IG cycles, especially at glacial terminations. An enhanced supply of southern sourced O_2-rich water drove the significant dissolved O_2 peaks during glacial terminations (Fig. 5B, C). Evidence with other features of AAIW also indicates the increased SO upwelling and AAIW advection into the low-latitude thermocline during glacial terminations, such as $\Delta^{14}C$ record from the southeast Pacific (Siani et al., 2013), opal peaks at low-latitudes (Hendry et al., 2012; Meckler et al., 2013), Nd isotope record from the Tobago Basin and East Equatorial Pacific (Pahnke et al., 2008; Pena et al., 2013), widespread minimum in $\delta^{13}C$ of tropical planktonic foraminifera (Spero et al., 2002), and the $\delta^{13}C$ record of atmospheric CO_2 derived from the Taylor Dome ice core (Smith et al., 1999). These records have been interpreted to represent an enhanced SO ventilation and southern sourced O_2 supply to support the "deglacial ventilation hypothesis" (Anderson et al., 2009; Martínez-Botí et al., 2015). In addition to SO ventilation, geochemical proxies and model results suggest that enhanced deglacial NPIW formation could transport more dissolved O_2 to the WTP

thermocline (Zou et al., 2020; Menviel et al., 2018). Furthermore, our deglacial dissolved O_2 peaks, consistent with the deglacial ventilation hypothesis, follow the deep-water carbonate ion concentration reconstruction from the same core (Qin et al., 2018).

The SO ventilation has the potential to primarily control the dissolved O_2 in the WTP thermocline during G–IG cycles, especially at glacial terminations. For example, freshwater injection owing to the North Atlantic/Arctic ice sheet retreat, supported by ice-rafted debris record in the North Atlantic (Fig.5; Barker et al., 2015; Wright et al., 2002), induced a cessation of the Atlantic meridional overturning circulation (Zhang et al., 2013). This process and the Antarctic local orbital forcing (Laepple et al., 2011; WAIS, 2013) might together trigger sea-ice decline (Wolff et al., 2006; Stephens et al., 2000) and a southward movement/enhancement of the Southern Hemisphere westerlies (Fig. 5D; Law et al., 2008; Toggweiler et al., 2008; Govin et al., 2009; Anderson et al., 2009), which enhanced the SO upwelling (Anderson et al., 2009; Marshall et al., 2012). Simultaneously, the Atlantic meridional overturning circulation cessation could enhance NPIW formation (Zou et al., 2020; Menviel et al., 2018).

Consequently, improved ventilation in the southern/northern higher-latitude water masses could lead to the O_2-rich water upwelling and feeding the WTP thermocline. We conclude that AAIW advection dominates these physical processes with a minor contribution from the NPIW.

4. Large-amplitude variation in dissolved O_2 during MIS 13 to 11

The most significant characteristic in the WTP TO during the last 700 kyr is the largest amplitude variations during MIS 13-11, the value of which rose from minimum to maximum (Fig. 5B). MIS 13 was the weakest interglacial of the last 800 kyr (Lang & Wolff, 2011; PAGES, 2016), with cooler Antarctic temperatures (Jouzel et al., 2007), more SO sea-ice cover (Wolff et al., 2006), a northward movement/weakening of the Southern Hemisphere westerlies (Fig. 5D; WAIS, 2013), and lower CO_2 and CH_4 concentrations than those recorded in the preceding and subsequent interglacials (Loulergue et al., 2008; Luthi et al., 2008). Our records imply that a weaker SO ventilation during MIS 13, associated with a weaker interglacial/lower pCO_2 (Fig. 5), may partially explain the relatively low dissolved O_2 to the low-latitude thermocline.

Subsequently, the reconstructed dissolved O_2 reached its maximum during the early part of MIS 11 following the largest amplitude variation during the last 700 kyr (Fig. 5B). This period covered the mid-Brunhes climatic shift as a major step change in global climate conditions (Droxler et al., 2003), completing the transition from the lukewarm interglacials to recent interglacials. In MIS 11, atmospheric pCO_2 reached ~280 ppmv, for the first time, from the previous interglacials below 260 ppmv (Luthi et al., 2008). The dome-like high atmospheric pCO_2 caused MIS 11 to have an unusually long and strong interglacial period (Droxler et al., 2003). The largest amplitude increase of the dissolved O_2 from minimum to maximum, closely related to the SO ventilation, corresponds to the climate transition covering the mid-Brunhes climatic shift. This may imply significant changes in the SO process, which requires further

confirmation with longer records of SO ventilation with direct proxies, as current records are no older than the mid-Brunhes.

The TO decreased rapidly after reaching the maxima during early MIS 11, to a very low value at ~390 ka B.P. (Fig. 5B). Simultaneously, the widespread carbonate dissolution during the mid-Brunhes dissolution interval is best explained by an increase in pelagic carbonate production due to coccolithophore blooms (Barker et al., 2006), triggering an increased organic carbon export flux owing to the ballast mineral effect. At the same time, the rapid weakening of SO ventilation and increased export productivity could explain the low value of oxygen via combined physical and biological processes (Fig. 4C, 5C). The increased organic carbon export supports the explanation from Barker et al. (2006); in addition, the establishment of the SO stratification would benefit CO_2 sequestration in deep carbon reservoirs.

The consistent and simultaneous dramatic increments during MIS 13 to 11 and the following low oxygenation during the mid-Brunhes dissolution interval, support a close coupling between the global mid-Brunhes climatic shift scenario of SO ventilation and tropical thermocline oxygenation.

Conclusions

We reconstructed the dissolved O_2 levels in the Western Tropical Pacific (WTP) thermocline during the last 700 kyr using the relative abundance of the thermocline species/resistant species stack extracted from Core MD06-3047. Our results yielded the following conclusions:

(1) The dissolved O_2 in the WTP thermocline shows significant periodicity during glacial–interglacial cycles over the last 700 kyr. In most glacial periods, the thermocline oxygenation became gradually enhanced. During glacial terminations, the significant relative abundance of thermocline-dwelling species minimum events reflect the remarkably dome-like enhanced oxygenation of the thermocline.

(2) The remote physical process of lateral O_2 advection (dominated by Southern Ocean (SO) ventilation and Antarctic Intermediate Water advection, with a minor contribution of North Pacific Intermediate Water (NPIW)) and the local biological process of O_2 consumption (by organic biological productivity, determined by iron supply and NPIW-driven nutrient supply) may together control the WTP thermocline oxygenation on glacial–interglacial cycles. Furthermore, the surprisingly synchronous co-variation indicates that SO ventilation and Antarctic Intermediate Water advection have the potential to primarily control the dissolved O_2 in the WTP thermocline on glacial–interglacial cycles, especially during glacial terminations.

(3) The consistent and simultaneous dramatic increments during MIS13-11 transiton and each deglacial period, and the very low oxygenation during the mid-Brunhes dissolution interval, provide robust support for a close coupling between the global (mid-Brunhes) climatic shift scenario of SO ventilation and WTP thermocline oxygenation.

Declaration of Competing Interest

The authors declare that they have no known competing financial interests or personal relationships that could have appeared to influence the work reported in this paper.

Acknowledgments

This work was supported by National Natural Science Foundation of China (NSFC, grant nos. 41830539 and 41976080), Evaluation and Effect of Paleoclimatic Evolution (grant no. GASI-04-QYQH-04), and Taishan Scholars Project Funding (grant no. ts20190963).

References

Anderson, R., Ali, S., Bradtmiller, L., Nielsen, S., Fleisher, M., Anderson, B., Burckle, L., 2009. Wind-driven upwelling in the Southern Ocean and the deglacial rise in atmospheric CO_2. Science 323, 1443-1448.

Barker, S., Archer, D., Booth, L., Elderfield, H., Henderiks, J., Rickaby, R.E.M., 2006. Globally increased pelagic carbonate production during the Mid-Brunhes dissolution interval and the CO_2 paradox of MIS 11. Quaternary Science Reviews 25, 3278-3293.

Barker, S., Chen, J., Gong, X., Jonkers, L., Knorr, G., Thornalley, D., 2015. Icebergs not the trigger for North Atlantic cold events. Nature 520, 333-336.

Bazin, L., Landais, A., Lemieux-Dudon, B., Toyé Mahamadou Kele, H., Veres, D., Parrenin, F., Martinerie, P., Ritz, C., Capron, E., Lipenkov, V., 2013. An optimized multi-proxy, multi-site Antarctic ice and gas orbital chronology (AICC2012): 120–800 ka. Climate of the Past 9, 1715-1731.

Berger, W.H., 1975. Deep-sea carbonates: dissolution profiles from foraminiferal preservation, in: Sliter, W.V., Bé, A.W.H., Berger, W.H. (Eds.), Dissolution of Deep-sea Carbonates. Cushman Foundation for Foraminiferal Research.

Berger, W.H., Adelseck, C.G., Jr., Mayer, L.A., 1976. Distribution of Carbonate in Surface Sediments of the Pacific Ocean. J. Geophys. Res. 81, 2617-2627.

Bostock, H.C., Opdyke, B.N., Williams, M.J., 2010. Characterising the intermediate depth waters of the Pacific Ocean using $\delta^{13}C$ and other geochemical tracers. Deep Sea Research Part I: Oceanographic Research Papers 57, 847-859.

Bostock, H.C., Sutton, P.J., Williams, M.J., Opdyke, B.N., 2013. Reviewing the circulation and mixing of Antarctic Intermediate Water in the South Pacific using evidence from geochemical tracers and Argo float trajectories. Deep Sea

Research Part I: Oceanographic Research Papers 73, 84-98.

Bradtmiller, L.I., Anderson, R.F., Sachs, J.P., Fleisher, M.Q., 2010. A deeper respired carbon pool in the glacial equatorial Pacific Ocean. Earth and Planetary Science Letters 299, 417-425.

Chen, S., Li, T., Tang, Z., Qiu, X., Xiong, Z., Nan, Q., Xu, Z., Chang, F., 2011. Response of the northwestern Pacific upper water $d^{13}C$ to the last deglacial ventilation of the deep Southern Ocean. Chinese Science Bulletin 56, 2628-2634.

Cullen, J.L., 1981. Microfossil evidence for changing salinity patterns in the Bay of Bengal over the last 20 000 years. Palaeogeography, Palaeoclimatology, Palaeoecology 35, 315-356.

Curry, W.B., Lohmann, G., 1982. Carbon isotopic changes in benthic foraminifera from the western South Atlantic: Reconstruction of glacial abyssal circulation patterns. Quaternary Research 18, 218-235.

Droxler, A.W., Alley, R. B., Howard, W. R., Poore, R. Z., & Burckle, L. H., 2003. Unique and exceptionally long interglacial Marine Isotope Stage 11: Window into Earth warm future climate. Earth's Climate and Orbital Eccentricity: The Marine Isotope Stage 11 Question.

Dugdale, R., Wischmeyer, A., Wilkerson, F., Barber, R., Chai, F., Jiang, M.-S., Peng, T.-H., 2002. Meridional asymmetry of source nutrients to the equatorial Pacific upwelling ecosystem and its potential impact on ocean–atmosphere CO2 flux; a data and modeling approach. Deep Sea Research Part II: Topical Studies in Oceanography 49, 2513-2531.

Fairbanks, R.G., Sverdlove, M., Free, R., Wiebe, P.H., Be, A.W.H., 1982. Vertical distribution and isotopic fractionation of living planktonic foraminifera from the Panama Basin. Nature 298, 841-844.

FAIRBANKS, R.G., WIEBE, P.H., BE, A.W.H., 1980. Vertical Distribution and Isotopic Composition of Living Planktonic Foraminifera in the Western North Atlantic. Science 207, 61-63.

Faul, K.L., Ravelo, A.C., Delaney, M., 2000. Reconstructions of upwelling, productivity, and photic zone depth in the eastern equatorial Pacific Ocean using planktonic foraminiferal stable isotopes and abundances. The Journal of Foraminiferal Research 30, 110-125.

Feely, R.A., Boutin, J., Cosca, C.E., Dandonneau, Y., Etcheto, J., Inoue, H.Y., Ishii, M., Le Quéré, C., Mackey, D.J., McPhaden, M., 2002. Seasonal and interannual variability of CO2 in the equatorial Pacific. Deep Sea Research Part II: Topical Studies in Oceanography 49, 2443-2469.

Garcia, H., Weathers, K., Paver, C., Smolyar, I., Boyer, T., Locarnini, M., Zweng, M., Mishonov, A., Baranova, O., Seidov, D., 2019. World Ocean Atlas 2018, Volume 3: Dissolved Oxygen, Apparent Oxygen Utilization, and Dissolved Oxygen Saturation.

Govin, A., Michel, E., Labeyrie, L., Waelbroeck, C., Dewilde, F., Jansen, E., 2009. Evidence for northward expansion of Antarctic Bottom Water mass in the Southern Ocean during the last glacial inception. Paleoceanography 24.

Guo, J., Qiu, X., Algeo, T.J., Li, T., Xiong, Z., Zhao, D., Dang, H., Qiao, P., Qin, B., Jia, Q., 2022. Precession-driven changes in air-sea CO2 exchange by East Asian summer monsoon in the Western Tropical Pacific since MIS 6. Palaeogeography, Palaeoclimatology, Palaeoecology 607, 111267.

Hartin, C.A., Fine, R.A., Sloyan, B.M., Talley, L.D., Chereskin, T.K., Happell, J., 2011. Formation rates of Subantarctic Mode Water and Antarctic Intermediate Water within the South Pacific. Deep Sea Research Part I: Oceanographic Research Papers 58, 524-534.

Hemleben, C., Spindler, M., Anderson, O.R., 2012. Modern planktonic foraminifera. Springer Science & Business Media.

Hendry, K.R., Robinson, L.F., 2012. The relationship between silicon isotope fractionation in sponges and silicic acid concentration: modern and core-top studies of biogenic opal. Geochimica et Cosmochimica Acta 81, 1-12.

Hilde, T.W., Chao-Shing, L., 1984. Origin and evolution of the West Philippine Basin: a new interpretation. Tectonophysics 102, 85-104.

Jaccard, S., Galbraith, E., Sigman, D.M., Haug, G., 2010. A pervasive link between Antarctic ice core and subarctic Pacific sediment records over the past 800 kyrs. Quaternary Science Reviews 29, 206-212.

Jaccard, S.L., Galbraith, E.D., 2012. Large climate-driven changes of oceanic oxygen concentrations during the last deglaciation. Nature Geoscience 5, 151-156.

Jaccard, S.L., Galbraith, E.D., Sigman, D.M., Haug, G.H., Francois, R., Pedersen, T.F., Dulski, P., Thierstein, H.R., 2009. Subarctic Pacific evidence for a glacial deepening of the oceanic respired carbon pool. Earth and Planetary Science Letters 277, 156-165.

Jaccard, S.L., Hayes, C.T., Martínez-García, A., Hodell, D.A., Anderson, R.F., Sigman, D.M., Haug, G.H., 2013. Two Modes of Change in Southern Ocean Productivity Over the Past Million Years. Science 339, 1419-1423.

Jacobel, A., Anderson, R., Winckler, G., Costa, K., Gottschalk, J., Middleton, J., Pavia, F., Shoenfelt, E., Zhou, Y., 2019. No evidence for equatorial Pacific dust fertilization. Nature Geoscience 12, 154-155.

Jansen, J., Kuijpers, A., Troelstra, S., 1986. A mid-Brunhes climatic event: Long-term changes in global atmosphere and ocean circulation. Science 232, 619-622.

Jia, Q., Li, T., Xiong, Z., Chang, F., 2015. Foraminiferal carbon and oxygen isotope composition characteristics and the paleoceanographic implications in the north margin of the Western Pacific Warm Pool over the past about 700,000 years. Quaternary Science 035, 401-410.

Jia, Q., Li, T., Xiong, Z., Steinke, S., Algeo, T.J., Jiang, F., Chang, F., Qin, B., 2020. Thermocline dynamics in the northwestern tropical Pacific over the past 700 kyr. Quaternary Science Reviews 244, 106465.

Jouzel, J., Masson-Delmotte, V., Cattani, O., Dreyfus, G., Falourd, S., Hoffmann, G., Minster, B., Nouet, J., Barnola, J.-M., Chappellaz, J., 2007. Orbital and millennial Antarctic climate variability over the past 800,000 years. Science 317, 793-796.

Karstensen, J., Stramma, L., Visbeck, M., 2008. Oxygen minimum zones in the eastern tropical Atlantic and Pacific oceans. Progress in Oceanography 77, 331-350.

Laepple, T., Werner, M., Lohmann, G., 2011. Synchronicity of Antarctic temperatures and local solar insolation on orbital timescales. Nature 471, 91-94.

Lang, N., Wolff, E.W., 2011. Interglacial and glacial variability from the last 800 ka in marine, ice and terrestrial archives. Climate of the Past 7, 361-380.

Law, R.M., Matear, R.J., Francey, R.J., 2008. Comment on "Saturation of the Southern Ocean CO2 Sink Due to Recent Climate Change". Science 319, 570-570.

Lisiecki, L.E., Raymo, M.E., 2005. A Pliocene-Pleistocene stack of 57 globally distributed benthic δ18O records. Paleoceanography 20, PA1003.

Liu, Z., Zhao, Y., Colin, C., Siringan, F.P., Wu, Q., 2009. Chemical weathering in Luzon, Philippines from clay mineralogy and major-element geochemistry of river sediments. Applied Geochemistry 24, 2195-2205.

Loulergue, L., Schilt, A., Spahni, R., Masson-Delmotte, V., Blunier, T., Lemieux, B., Barnola, J.-M., Raynaud, D., Stocker, T.F., Chappellaz, J., 2008. Orbital and millennial-scale features of atmospheric CH4 over the past 800,000 years. Nature 453, 383-386.

Luthi, D., Le Floch, M., Bereiter, B., Blunier, T., Barnola, J.-M., Siegenthaler, U., Raynaud, D., Jouzel, J., Fischer, H., Kawamura, K., Stocker, T.F., 2008. High-resolution carbon dioxide concentration record 650,000-800,000 years before

present. Nature 453, 379-382.

Marshall, J., Speer, K., 2012. Closure of the meridional overturning circulation through Southern Ocean upwelling. Nature Geoscience.

Martínez-Botí, M.A., Marino, G., Foster, G.L., Ziveri, P., Henehan, M.J., Rae, J.W.B., Mortyn, P.G., Vance, D., 2015. Boron isotope evidence for oceanic carbon dioxide leakage during the last deglaciation. Nature 518, 219-222.

Matsumoto, K., Sarmiento, J.L., 2008. A corollary to the silicic acid leakage hypothesis. Paleoceanography 23.

Max, L., Rippert, N., Lembke-Jene, L., Mackensen, A., Nürnberg, D., Tiedemann, R., 2017. Evidence for enhanced convection of North Pacific Intermediate Water to the low-latitude Pacific under glacial conditions. Paleoceanography 32, 41-55.

McManus, J.F., Oppo, D.W., Cullen, J.L., 1999. A 0.5-million-year record of millennial-scale climate variability in the North Atlantic. Science 283, 971-975.

Meckler, A., Sigman, D., Gibson, K., François, R., Martínez-García, A., Jaccard, S., Röhl, U., Peterson, L., Tiedemann, R., Haug, G., 2013. Deglacial pulses of deep-ocean silicate into the subtropical North Atlantic Ocean. Nature 495, 495-498.

Members, W.D.P., 2013. Onset of deglacial warming in West Antarctica driven by local orbital forcing. Nature 500, 440-444.

Menviel, L., Spence, P., Yu, J., Chamberlain, M.A., Matear, R.J., Meissner, K.J., England, M.H., 2018. Southern Hemisphere westerlies as a driver of the early deglacial atmospheric CO_2 rise. Nature Communications 9, 2503.

Nameroff, T., Calvert, S., Murray, J., 2004. Glacial-interglacial variability in the eastern tropical North Pacific oxygen minimum zone recorded by redox-sensitive trace metals. Paleoceanography 19.

Ninnemann, U.S., Charles, C.D., 2002. Changes in the mode of Southern Ocean circulation over the last glacial cycle revealed by foraminiferal stable isotopic variability. Earth and Planetary Science Letters 201, 383-396.

Past Interglacials Working Group of PAGES., 2016. Interglacials of the last 800,000 years. Reviews of Geophysics 54, 162-219.

Pahnke, K., Goldstein, S.L., Hemming, S.R., 2008. Abrupt changes in Antarctic Intermediate Water circulation over the past 25,000 years. Nature Geoscience 1, 870-874.

Pena, L., Goldstein, S.L., Hemming, S.R., Jones, K.M., Calvo, E., Pelejero, C., Cacho, I., 2013. Rapid changes in meridional advection of Southern Ocean intermediate waters to the tropical Pacific during the last 30 kyr. Earth and Planetary Science Letters 368, 20-32.

Pena, L.D., Cacho, I., Ferretti, P., Hall, M.A., 2008. El Niño-Southern Oscillation-like variability during glacial terminations and interlatitudinal teleconnections. Paleoceanography 23, PA3101.

Petit, J.R., Jouzel, J., Raynaud, D., Barkov, N.I., Barnola, J.M., Basile, I., Bender, M., Chappellaz, J., Davis, M., Delaygue, G., Delmotte, M., Kotlyakov, V.M., Legrand, M., Lipenkov, V.Y., Lorius, C., Pepin, L., Ritz, C., Saltzman, E., Stievenard, M., 1999. Climate and atmospheric history of the past 420,000 years from the Vostok ice core, Antarctica. Nature 399, 429-436.

Pichevin, L.E., Reynolds, B.C., Ganeshram, R.S., Cacho, I., Pena, L., Keefe, K., Ellam, R.M., 2009. Enhanced carbon pump inferred from relaxation of nutrient limitation in the glacial ocean. Nature 459, 1114-1117.

Prell, W., Martin, A., Cullen, J., Trend, M., 1999. The Brown University Foraminiferal Data Base (BFD). PANGAEA https://doi. org/10.1594/pangaea 96900.

Qin, B., Li, T., Xiong, Z., Algeo, T., Jia, Q., 2018. Deep-Water Carbonate Ion Concentrations in the Western Tropical Pacific Since the Mid-Pleistocene: A Major Perturbation During the Mid-Brunhes. Journal of Geophysical Research: Oceans 123, 6876-6892.

Ravelo, A.C., Fairbanks, R.G., 1992. Oxygen Isotopic Composition of Multiple Species of Planktonic Foraminifera: Recorders of the Modern Photic Zone Temperature Gradient. Paleoceanography 7, 815-831.

Rippert, N., Max, L., Mackensen, A., Cacho, I., Povea, P., Tiedemann, R., 2017. Alternating Influence of Northern Versus Southern-Sourced Water Masses on the Equatorial Pacific Subthermocline During the Past 240 ka. Paleoceanography 32, 1256-1274.

Russell, J., Dickson, A., 2003. Variability in oxygen and nutrients in South Pacific Antarctic intermediate water. Global biogeochemical cycles 17.

Russell, J.L., Dixon, K.W., Gnanadesikan, A., Stouffer, R.J., Toggweiler, J., 2006. The Southern Hemisphere westerlies in a warming world: Propping open the door to the deep ocean. Journal of Climate 19, 6382-6390.

Sarmiento, J., Gruber, N., Brzezinski, M., Dunne, J., 2004. High-latitude controls of thermocline nutrients and low latitude biological productivity. Nature 427, 56-60.

Schlitzer, R., 2020. Ocean Data View, https://odv.awi.de.

Sexton, P.F., Norris, R.D., 2011. High latitude regulation of low latitude thermocline ventilation and planktic foraminifer populations across glacial–interglacial cycles. Earth and Planetary Science Letters 311, 69-81.

Shao, J., Stott, L.D., Menviel, L., Ridgwell, A., Ödalen, M., Mohtadi, M., 2020. The Atmospheric Bridge Communicated the $\delta^{13}C$ Decline during the Last Deglaciation to the Global Upper Ocean. Climate of the Past Discussions 2020, 1-28.

Siani, G., Michel, E., De Pol-Holz, R., DeVries, T., Lamy, F., Carel, M., Isguder, G., Dewilde, F., Lourantou, A., 2013. Carbon isotope records reveal precise timing of enhanced Southern Ocean upwelling during the last deglaciation. Nature communications 4.

Siegenthaler, U., Stocker, T.F., Monnin, E., Lüthi, D., Schwander, J., Stauffer, B., Raynaud, D., Barnola, J.-M., Fischer, H.,

Masson-Delmotte, V., Jouzel, J., 2005. Stable Carbon Cycle– Climate Relationship During the Late Pleistocene. Science 310, 1313-1317.

Sigman, D.M., Boyle, E.A., 2000. Glacial/interglacial variations in atmospheric carbon dioxide. Nature 407, 859-869.

Skinner, L.C., Fallon, S., Waelbroeck, C., Michel, E., Barker, S., 2010. Ventilation of the deep Southern Ocean and deglacial CO2 rise. Science 328, 1147-1151.

Smith, H.J., Fischer, H., Wahlen, M., Mastroianni, D., Deck, B., 1999. Dual modes of the carbon cycle since the Last Glacial Maximum. Nature 400, 248-250.

Spero, H.J., Lea, D.W., 2002. The Cause of Carbon Isotope Minimum Events on Glacial Terminations. Science 296, 522-525.

Stocker, T.F., Johnsen, S.J., 2003. A minimum thermodynamic model for the bipolar seesaw. Paleoceanography 18, 1087.

Stott, L., Timmermann, A., Thunell, R., 2007. Southern Hemisphere and deep-sea warming led deglacial atmospheric CO_2 rise and tropical warming. science 318, 435-438.

Talley, L.D., 2013. Closure of the global overturning circulation through the Indian, Pacific, and Southern Oceans: Schematics and transports. Oceanography 26, 80-97.

Tang, Z., Li, T., Chang, F., Nan, Q., Li, Q., 2013. Paleoproductivity evolution in the West Philippine Sea during the last 700 ka. Chinese Journal of Oceanology and Limnology 31, 435-444.

Tang, Z., Li, T., Xiong, Z., Dang, H., Guo, J., 2022. Covariation of Deep Antarctic Pacific Oxygenation and Atmospheric CO2 during the Last 770 kyr. Lithosphere 2022.

Tang, Z., Shi, X., Zhang, X., Chen, Z., Chen, M.-T., Wang, X., Wang, H., Liu, H., Lohmann, G., Li, P., Ge, S., Huang, Y., 2016. Deglacial biogenic opal peaks revealing enhanced Southern Ocean upwelling during the last 513 ka. Quaternary International 425, 445-452.

Thompson, P.R., Be, A.W.H., Duplessy, J.-C., Shackleton, N.J., 1979. Disappearance of pink-pigmented *Globigerinoides ruber* at 120,000 yr BP in the Indian and Pacific Oceans. Nature 280, 554-558.

Toggweiler, J., Dixon, K., Broecker, W., 1991. The Peru upwelling and the ventilation of the South Pacific thermocline. Journal of Geophysical Research: Oceans 96, 20467-20497.

Toggweiler, J.R., Russell, J., 2008. Ocean circulation in a warming climate. Nature 451, 286-288.

Tsuchiya, M., Lukas, R., Fine, R.A., Firing, E., Lindstrom, E., 1989. Source waters of the Pacific Equatorial Undercurrent. Progress in Oceanography 23, 101-147.

Turk, D., Lewis, M.R., Harrison, G.W., Kawano, T., Asanuma, I., 2001. Geographical distribution of new production in the western/central equatorial Pacific during El Niño and non-El Niño conditions. Journal of Geophysical Research: Oceans 106, 4501-4515.

Wan, S., Yu, Z., Clift, P.D., Sun, H., Li, A., Li, T., 2012. History of Asian eolian input to the West Philippine Sea over the last one million years. Palaeogeography, Palaeoclimatology, Palaeoecology 326-328, 152-159.

Watkins, J.M., Mix, A.C., Wilson, J., 1996. Living planktic foraminifera in the central tropical Pacific Ocean: Articulating the equatorial 'cold tongue' during La Niña, 1992. Marine Micropaleontology 33, 157-174.

Winckler, G., Anderson, R.F., Jaccard, S.L., Marcantonio, F., 2016. Ocean dynamics, not dust, have controlled equatorial Pacific productivity over the past 500,000 years. Proceedings of the National Academy of Sciences 113, 6119-6124.

Wolff, E.W., Fischer, H., Fundel, F., Ruth, U., Twarloh, B., Littot, G.C., Mulvaney, R., Röthlisberger, R., de Angelis, M., Boutron, C.F., Hansson, M., Jonsell, U., Hutterli, M.A., Lambert, F., Kaufmann, P., Stauffer, B., Stocker, T.F., Steffensen, J.P., Bigler, M., Siggaard-Andersen, M.L., Udisti, R., Becagli, S., Castellano, E., Severi, M., Wagenbach, D., Barbante, C., Gabrielli, P., Gaspari, V., 2006. Southern Ocean sea-ice extent, productivity and iron flux over the past eight glacial

cycles. Nature 440, 491-496.

Wright, A.K., Flower, B.P., 2002. Surface and deep ocean circulation in the subpolar North Atlantic during the mid-Pleistocene revolution. Paleoceanography 17, 20-21-20-16.

Wyrtki, K., 1962. The oxygen minima in relation to ocean circulation, Deep Sea Research and Oceanographic Abstracts. Elsevier, pp. 11-23.

Xiong, Z., Li, T., Crosta, X., Algeo, T., Chang, F., Zhai, B., 2013. Potential role of giant marine diatoms in sequestration of atmospheric CO2 during the Last Glacial Maximum: $\delta^{13}C$ evidence from laminated *Ethmodiscus rex* mats in tropical West Pacific. Global and Planetary Change 108, 1-14.

Xiong, Z., Li, T., Hönisch, B., Algeo, T.J., Bradtmiller, L., Cang, M., Laj, C., Wang, F., Lu, Z., Qin, B., 2022. Monsoon-and ENSO-driven surface-water pCO_2 variation in the tropical West Pacific since the Last Glacial Maximum. Quaternary Science Reviews 289, 107621.

Xu, Z., Li, A., Jiang, F., Xu, F., 2008. Geochemical character and material source of sediments in the eastern Philippine Sea. Chinese Science Bulletin 53, 923-931.

Xu, Z., Li, T., Clift, P.D., Liu, L., Wan, S., Chen, H., Tang, Z., Jiang, F., Xiong, Z., 2015. Quantitative estimates of Asian dust input to the western Philippine Sea in the mid-late Quaternary and its potential significance for paleoenvironment. Geochemistry, Geophysics, Geosystems 16, 3182-3196.

Xu, Z., Li, T., Wan, S., Nan, Q., Li, A., Chang, F., Jiang, F., Tang, Z., 2012. Evolution of East Asian monsoon: Clay mineral evidence in the western Philippine Sea over the past 700kyr. Journal of Asian Earth Sciences 60, 188-196.

Zhang, X., Lohmann, G., Knorr, G., Xu, X., 2013. Different ocean states and transient characteristics in Last Glacial Maximum simulations and implications for deglaciation. Clim. Past 9, 2319-2333.

Ziegler, M., Diz, P., Hall, I.R., Zahn, R., 2013. Millennial-scale changes in atmospheric CO_2 levels linked to the Southern Ocean carbon isotope gradient and dust flux. Nature Geoscience 6, 457-461.

Zou, J., Shi, X., Zhu, A., Kandasamy, S., Gong, X., Lembke-Jene, L., Chen, M.-T., Wu, Y., Ge, S., Liu, Y., 2020. Millennial-scale variations in sedimentary oxygenation in the western subtropical North Pacific and its links to North Atlantic climate. Climate of the Past 16, 387-407.

Figures

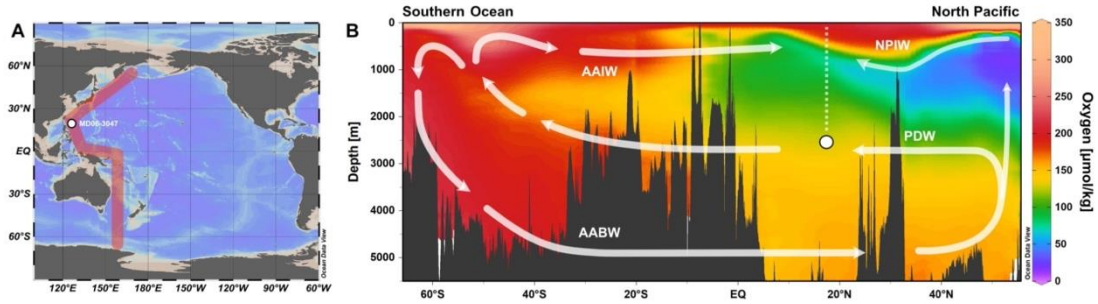

Fig. 1. Spatial variations in modern ocean oxygen concentrations and core location. (**A**) Map of the study core and the section location; (**B**) [O_2] (contours, in µmol/kg) in a meridional transect across the Pacific Ocean (Garcia et al., 2019). The **red shaded line** in (A) broadly represents the section location in (B). **White arrows** in (B) denote the general pathways of the overturning circuit. **PDW**: Pacific Deep Water; **AABW**: Antarctic Bottom Water; **AAIW**: Antarctic Intermediate Water; **NPIW**: North Pacific Intermediate Water. Core **MD06-3047** (white circle) is located in the tropical Western Pacific. The map was created using the **Ocean Data View** software (Schlitzer, 2020).

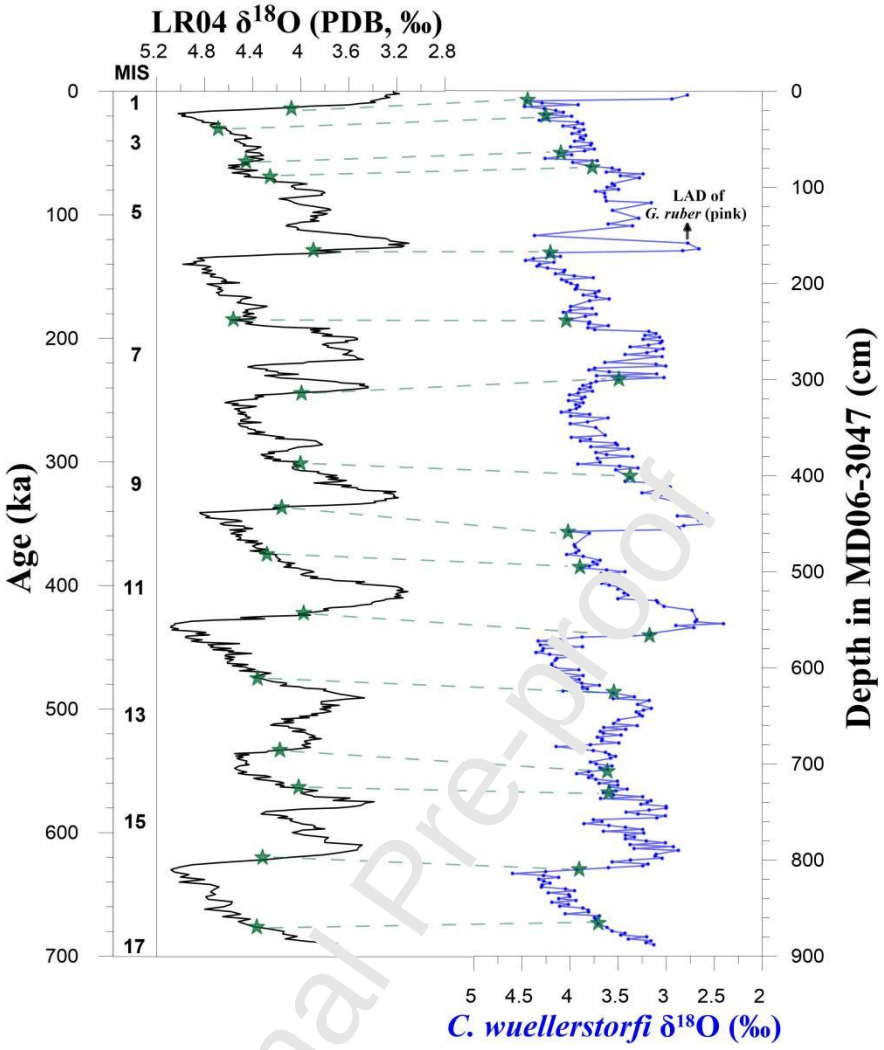

Fig. 2. Age model for core MD06-3047 (Tang et al., 2013), obtained by graphical comparison between the $\delta^{18}O$ record of epibenthic foraminifera *Cibicidoides wuellerstorfi* and the stacked global benthic LR04 $\delta^{18}O$ record (Lisiecki and Raymo, 2005), with additional refinement based on the last appearance datum (LAD) of *Globigerinoides ruber* (pink). Green stars represent oxygen-isotope events, and the black arrow indicates the LAD of *G. ruber* (pink).

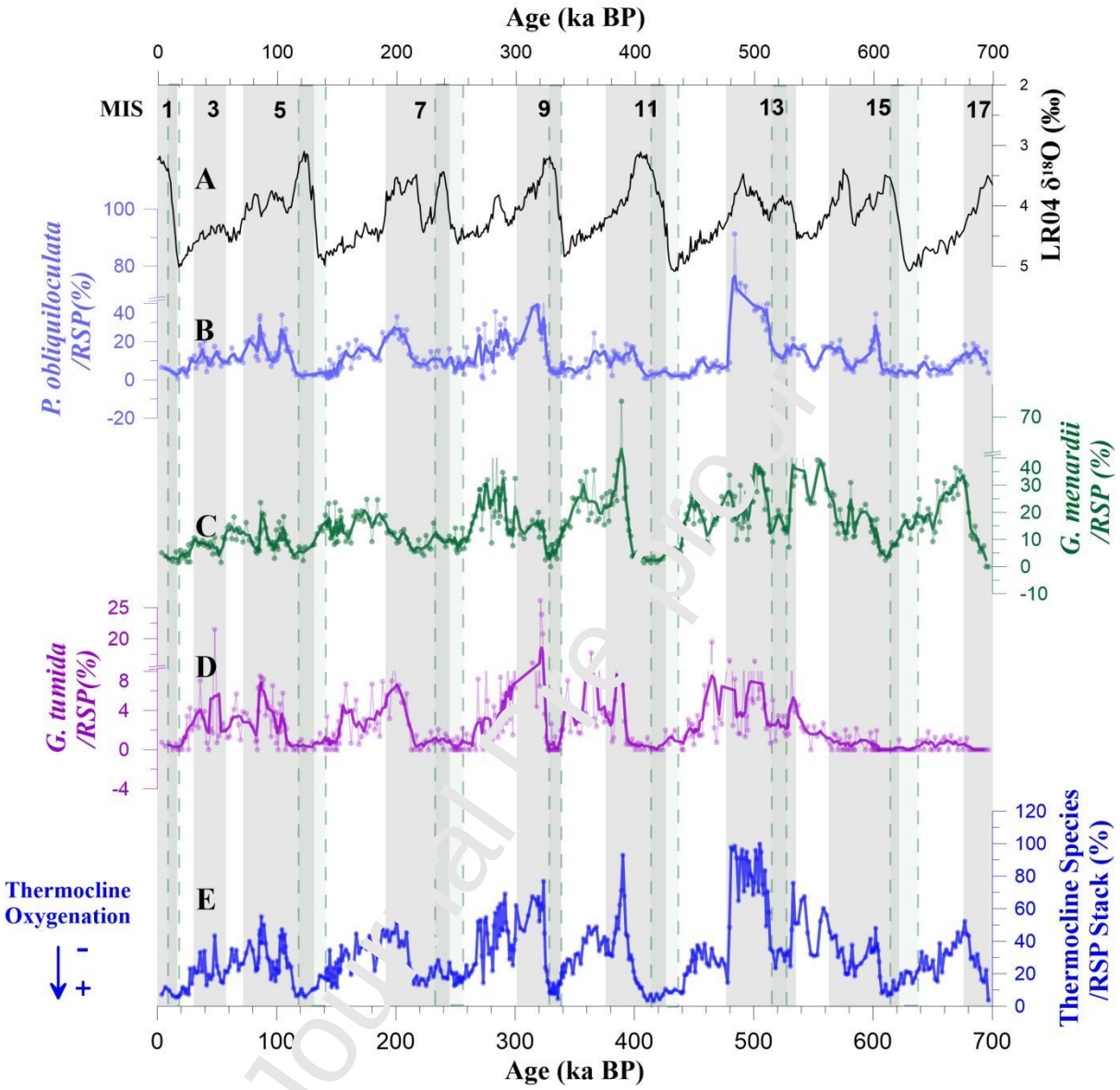

Fig. 3. (A) Record of stacked global benthic LR04 $\delta^{18}O$ (Lisiecki and Raymo, 2005). **(B)–(E)** The normative relative abundance of *P. obliquiloculata*/resistant species (RSP), *G. menardii*/RSP, *G. tumida*/RSP, and the three thermocline species stack/RSP (thermocline oxygenation, TO) from core MD06-3047. The lines are the three-point running average in **(B)**-**(D)**. The performed normalization calculations could minimize the effects of post-depositional dissolution. Grey shadings indicate interglacial periods; green shadings indicate deglacial periods / thermocline-dwelling species minimum events, characterized by very low relative abundance of thermocline-dwelling species, reflect the remarkably enhanced thermocline oxygenation. The arrow and plus signs indicates the direction of the enhanced process.

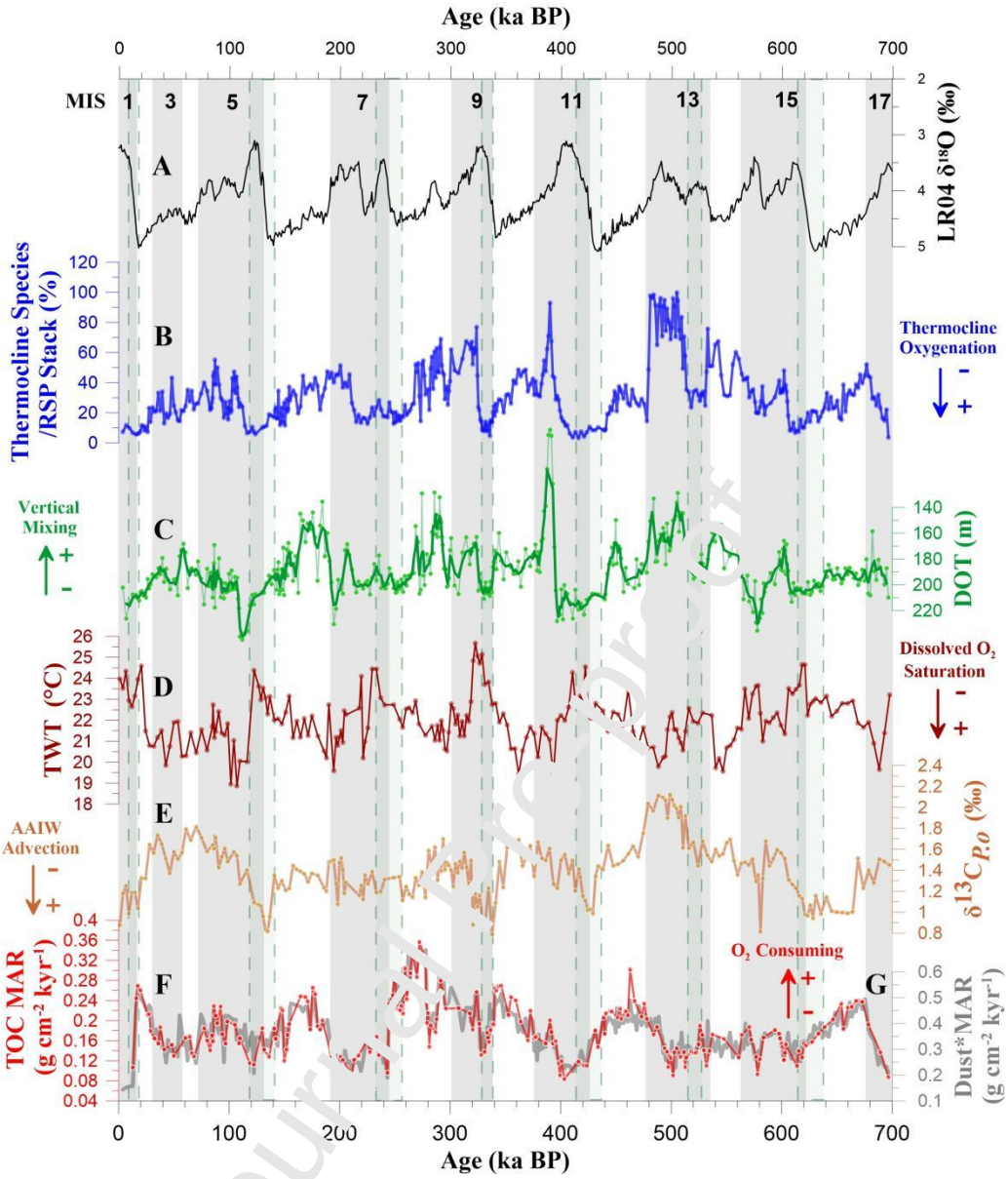

Fig. 4. (A) Record of stacked global benthic LR04 $\delta^{18}O$ (Lisiecki and Raymo, 2005). **(B)** The normative relative abundance of stacked thermocline species / resistant species (thermocline oxygenation, TO) from core MD06-3047. **(C)** Depth of thermocline (DOT) from core MD06-3047 (Tang et al., 2013). The green line is the three-point running average. **(D)** The thermocline water temperature (TWT) from core MD06-3047B is at the same location as the study core (Jia et al., 2020). **(E)** $\delta^{13}C$ of *P. obliquiloculata* from core MD06-3047B (Jia et al., 2015). **(F-G)** MARs of total organic carbon (TOC) and eolian dust from core MD06-3047 (Xu et al., 2015). Grey shadings indicate interglacial periods; green shadings indicate deglacial periods / thermocline-dwelling species minimum events, characterized by very low relative abundance of thermocline-

dwelling species, reflect the remarkably enhanced thermocline oxygenation. Arrows and plus signs indicate the direction of enhancement of various processes.

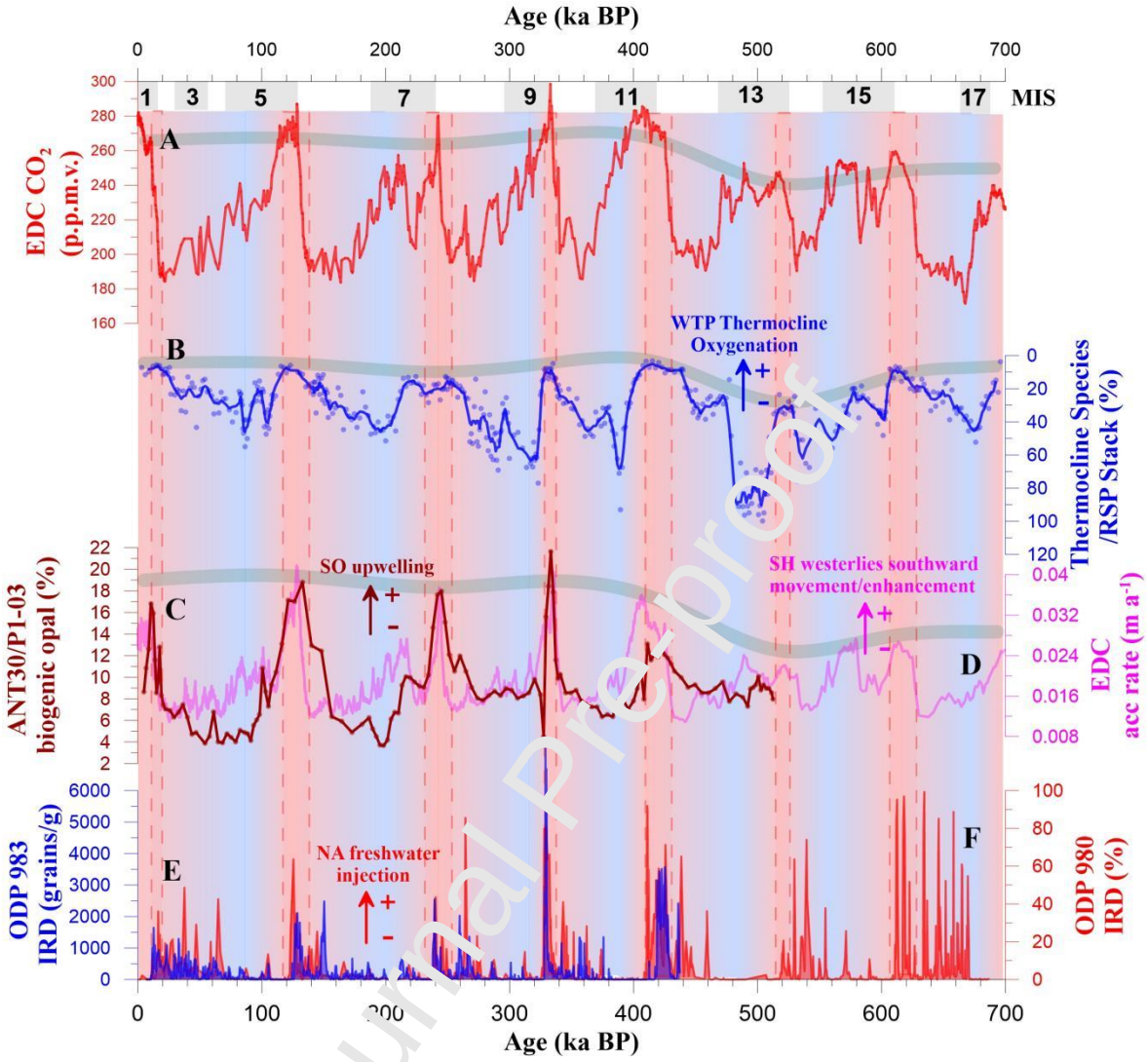

Fig. 5. (A) pCO_2 record from EPICA Dome C (EDC) (Siegenthaler et al., 2005). **(B)** The normative relative abundance of stacked thermocline species / resistant species (Thermocline Oxygenation, TO) from core MD06-3047. The blue line is the three-point running average. **(C)** Biogenic opal from core ANT29/P1-03, located in the Antarctic Zone of the Southern Indian Ocean (Tang et al., 2016). **(D)** Accumulation rate at EPICA Dome C (EDC) (Bazin et al., 2013). Ice-rafted debris (IRD) record from **(E)** ODP site 983 (McManus et al., 1999) and **(F)** ODP site 980 (Barker et al., 2015) in the northern Atlantic. The gradual red and blue shadings indicate the periodic higher and lower values in dissolved O_2 in the Western Tropical Pacific thermocline during glacial–interglacial cycles, respectively. The green shading curve shows the different interglacial states before and after MIS13. Red dashed frames indicate deglacial periods / thermocline-dwelling species minimum events, characterized by very

low relative abundance of thermocline-dwelling species, reflect the remarkably enhanced thermocline oxygenation. Arrows and plus signs indicate the direction of enhancement of various processes.

Declaration of Competing Interest

The authors declare that they have no known competing financial interests or personal relationships that could have appeared to influence the work reported in this paper.

Highlights:

- During glacial terminations, significant thermocline-dwelling species minimum events and dome-like enhanced oxygenation in the Western Tropical Pacific (WTP) thermocline have existed since at least ~700 ka.

- The remote physical (advection of oxygenated high latitude intermediate water) and the local biological (high productivity) processes may together control WTP thermocline oxygenation on glacial–interglacial cycles.

- Southern Ocean ventilation and the WTP thermocline oxygenation have a close coupling in global (mid-Brunhes) climatic shift scenario.